

Durham Research Online

Deposited in DRO:

12 October 2016

Version of attached file:

Published Version

Peer-review status of attached file:

Peer-reviewed

Citation for published item:

Dodd, Linzi E. and Geraldi, Nicasio R. and Xu, Ben B. and McHale, Glen and Wells, Gary G. and Stuart-Cole, Simone and Martin, James and Newton, Michael I. and Wood, David (2016) 'Low friction droplet transportation on a substrate with a selective Leidenfrost effect.', *ACS applied materials interfaces.*, 8 (34). pp. 22658-22663.

Further information on publisher's website:

<http://dx.doi.org/10.1021/acsami.6b06738>

Publisher's copyright statement:

This is an open access article published under a Creative Commons Attribution (CC-BY) License, which permits unrestricted use, distribution and reproduction in any medium, provided the author and source are cited.

Additional information:

Use policy

The full-text may be used and/or reproduced, and given to third parties in any format or medium, without prior permission or charge, for personal research or study, educational, or not-for-profit purposes provided that:

- a full bibliographic reference is made to the original source
- a [link](#) is made to the metadata record in DRO
- the full-text is not changed in any way

The full-text must not be sold in any format or medium without the formal permission of the copyright holders.

Please consult the [full DRO policy](#) for further details.

Low Friction Droplet Transportation on a Substrate with a Selective Leidenfrost Effect

Linzi E. Dodd* and David Wood

Microsystems Technology Group, School of Engineering & Computing Sciences, Durham University, Durham DH1 3LE, U.K.

Nicasio R. Geraldi, Gary G. Wells, Glen McHale, and Ben B. Xu

Smart Materials and Surfaces Lab, Faculty of Engineering and Environment, Northumbria University, Newcastle upon Tyne NE1 8ST, U.K.

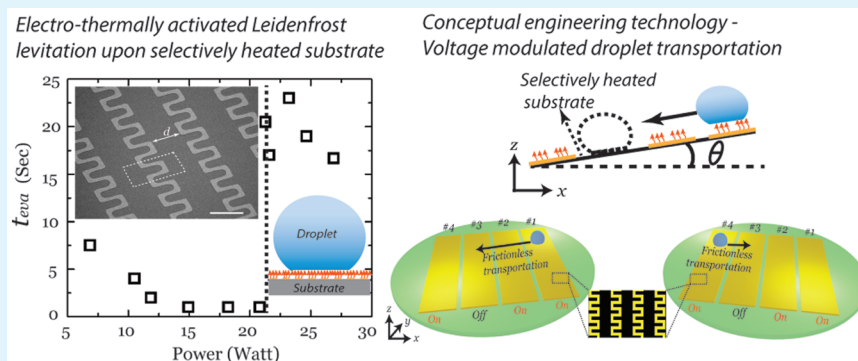
Simone Stuart-Cole and James Martin

Reece Innovation, Armstrong Works, Scotswood Road, Newcastle upon Tyne NE15 6UX, U.K.

Michael I. Newton

School of Science and Technology, Nottingham Trent University, Nottingham NG11 8NS, U.K.

Supporting Information



ABSTRACT: An energy saving Leidenfrost levitation method is introduced to transport microdroplets with virtually frictionless contact between the liquid and solid substrate. Through microengineering of the heating units, selective areas of the whole substrate can be electrothermally activated. A droplet can be levitated as a result of the Leidenfrost effect and further transported when the substrate is tilted slightly. Selective electroheating produces a uniform temperature distribution on the heating units within 1 s in response to a triggering voltage. Alongside these experimental observations, finite element simulations were conducted to understand the role of substrate thermal conductivity on the temperature profile of the selectively heated substrate. We also generated phase diagrams to verify the Leidenfrost regime for different substrate materials. Finally, we demonstrated the possibility of controlling low friction high speed droplet transportation (~ 65 mm/s) when the substrate is tilted ($\sim 7^\circ$) by structurally designing the substrate. This work establishes the basis for an entirely new approach to droplet microfluidics.

KEYWORDS: droplet transportation, Leidenfrost effect, selective heating, microengineering, MEMS

INTRODUCTION

Transporting droplets in a controllable and energy efficient manner could have a significant impact on several engineering applications, such as low drag liquid transportation,^{1,2} water collection,^{3,4} and advanced microfluidic devices.⁵ On the basis of a theoretical understanding of the wetting of surfaces, common approaches usually focus on creating a surface with designed physical/chemical features, e.g., hierarchical micro/

nanostructured surfaces,^{6,7} chemical gradients,^{8,9} or slippery surfaces created by infusing low surface tension lubricant into microstructures that yield directional motion of water droplets when tilted at a low angle.^{10–12} Notably, some interesting

Received: June 6, 2016

Accepted: August 2, 2016

Published: August 2, 2016



attempts have demonstrated liquid transportation efficiency using such techniques: for example, Chaudhury and Whitesides achieved an average velocity of 1–2 mm/s for droplet transportation on a silicon wafer possessing a gradient in wettability,¹³ Ghosh et al. employed extreme wettability patterns to achieve a flow rate of up to 300 mm/s,¹⁴ and Lv et al. achieved a maximum speed of 420 mm/s for droplet transportation in a microfluidic system.¹⁵ Approaches taken to date have been based on the liquid–solid contact, where the droplet motion will more or less be affected by the friction or dragging effect induced by local surface roughness, dimensional confinement, as well as the nonuniformity of the surface wettability.

The Leidenfrost phenomenon (Figure 1a), first discovered in 1756,¹⁶ describes a metastable state of a droplet on a substrate

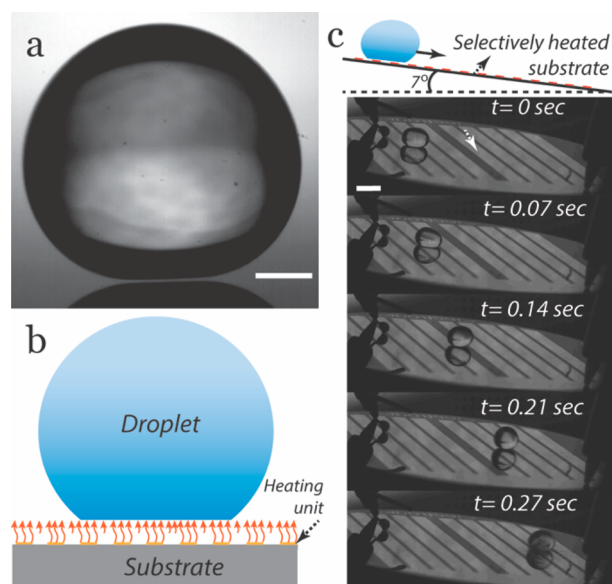


Figure 1. Initializing the Leidenfrost effect by creating localized Joule heating areas with selective coverage of heating units on a substrate. (a) Side-view image of a traditional Leidenfrost levitated water droplet on a heated silicon wafer surface ($\sim 300\text{ }^{\circ}\text{C}$); the scale bar is $500\text{ }\mu\text{m}$. (b) Schematic illustration of Leidenfrost levitation on a substrate selectively covered by metal heating units. (c) The concept is examined through virtually frictionless transportation of an isopropanol (IPA) droplet ($\sim 40\text{ }\mu\text{L}$) supported by the levitation vapor layer. The substrate is selectively covered by heating units in bands 2.5 mm in width (indicated by the white arrow), indicating droplet transportation speeds of $\sim 65\text{ mm s}^{-1}$; the substrate is tilted by 7° , and the scale bar is 2 mm .

heated significantly above the boiling point of the liquid. In this state, the droplet is levitated by an instantaneously generated vapor layer ($\sim 100\text{--}200\text{ }\mu\text{m}$) caused by the initial contact of the droplet with the substrate.^{17–21} The levitation yields a virtually frictionless contact between the droplet and substrate,^{21–23} therefore playing a key role in drag reduction for the liquid flow.^{24,25} Moreover, the vapor layer acts as a thermal insulator, preventing rapid droplet evaporation despite the high temperature of the substrate. Recent developments show some attempts to control the droplet motion based on Leidenfrost effect levitation by employing ratcheted and other patterned substrates,^{21,26–29} magnetic fields,³⁰ electric fields,³¹ and acoustic radiation pressure.³² However, the actuation of the Leidenfrost effect for a droplet has thus far involved heating the

entire substrate, which limits downstream applications due to the extreme substrate temperature condition. Despite recent work to reduce the transition temperature,^{24,28} the high energy consumption remains due to heating the substrate globally rather than the localized area which supports the droplet.

In this study, we trigger Leidenfrost levitation of a droplet by the application of a voltage to micrometer-scaled serpentine-shaped heating arrays, which cover the substrate in a selective manner. In addition to initializing levitation of droplets of three different liquids via selective heating of substrate areas, we also show that droplet transportation can be actuated and controlled by designing heating array patterns along with tilting of the substrate ($5\text{--}10^{\circ}$). The proposed strategy of selective heating could significantly reduce the energy input needed to actuate the Leidenfrost effect and also offer a control mechanism for droplet motion by locally controlling the designed heating array. When our approach is combined with surface relief patterns, precise directional control and self-propulsion can be achieved without the need to tilt the surface.³³ It also enables the possible integration of droplet levitation into microsystems as a new type of on-chip platform.

EXPERIMENTAL SECTION

Microfabrication. Thin-film resistors were fabricated on different substrates, i.e., borosilicate glass and silicon (with oxidation layer) wafers. After the substrate was cleaned, a thin-film metal layer ($\text{Cr}/\text{Au} = \sim 10/\sim 100\text{ nm}$ in thickness) was coated on the substrate via electron beam evaporation. The resistor patterns were photolithographically transferred onto the metal layer by a spinning Megaposit SPR-350 photoresist which was exposed to UV light in an EVG mask aligner and then developed in a Microposit MF-319 developer for 90 s. The excess metal out of the photoresist's protection was removed using selective gold ($4:1:8\text{ KI:I}_2:\text{H}_2\text{O}$) and chromium ($7:34:1\text{ Ce}(\text{NH}_4)_2(\text{NO}_3)_6:\text{HNO}_3:\text{H}_2\text{O}$) wet etches, leaving the required resistor patterns with varying distances between consecutive lines.

Leidenfrost Levitation Activation and Measurements. Each wafer was selectively covered by 4 two-dimensional arrays of devices, and electrical contact pads for each array were designed to enable independent control of the heating arrays. A customized rig was assembled with a stainless steel stage on an $x y z \theta$ manipulator to assist characterization. To maintain a uniform temperature within the stage, an mbed-controlled Peltier cooler with cooling pipes and a fan was mounted on the underside of the stage to stabilize the ambient conditions. Spring-loaded electrical contacts were then used to pass a current through each array in turn. To verify the effectiveness of the Leidenfrost levitation, we tested three different liquids: isopropanol (surface tension $\sim 20\text{ mN/m}$), acetone (surface tension $\sim 28\text{ mN/m}$), and deionized water (surface tension $\sim 72\text{ mN/m}$). All liquids produced similar results once they were heated beyond their respective Leidenfrost transition temperatures. In this paper, we present the summarized results for IPA as a typical case for the lowest surface tension liquid, which is the most difficult liquid when attempting to use material techniques to create a superliquid-repellent state. A $1000\times$ USB optical microscope was used to observe the arrays, and an FLIR A40 thermal camera was used to observe the temperature profile of the substrate. Different powers were applied to each heated array in turn, and the array was left for 1 min for the temperature to equalize.

Simulation. A “unit cell” device was also modeled in COMSOL Multiphysics software, which also included the substrate, stage, and effects of the Peltier cooling as boundary conditions. The COMSOL model involves parametrized substrate gaps between consecutive unit cells so that all heating ratios can be simulated automatically. The substrate on either side of the unit cell is related to the heated ratio with the end of the substrate being the halfway point between two unit cells, which is the coldest point in the array and therefore the region most likely to cause a collapse in the Leidenfrost vapor layer. All of the solid vertical boundaries in this model have a symmetry condition,

whereas the air has an outflow condition. Finally, the bottom of the stainless steel domain has a fixed temperature boundary condition (21 °C) to simulate the Peltier cooler placed underneath the stainless steel stage.

RESULTS AND DISCUSSION

In our experiments, the concept of selective electrothermally actuating Leidenfrost levitation is achieved by engineering millimeter-scale heating units on the substrate. The heating units covering the substrate are intended to create a uniform distribution of the thermal energy to trigger the Leidenfrost effect (Figure 1b), but in a selective manner only where this is needed to levitate a droplet. Different substrates (borosilicate glass and silicon) were used to determine the effect of the substrate's thermal conductivity on the power needed for the Leidenfrost effect to occur. Because the thermal conductivities for borosilicate and silicon are 1.14 and 1480 W/mK, respectively, these choices provide a difference of over 3 orders of magnitude with this parameter.³² The silicon substrates were electrically insulated via a 100 nm-thick silicon dioxide layer grown by furnace oxidation between the substrate and the heating array layer. In preliminary experiments, we confirmed that the Leidenfrost effect could be achieved with droplets of IPA, acetone, and deionized water. Once the Leidenfrost effect was triggered, virtually frictionless liquid transportation was expected on a pretilted substrate.

We first considered a substrate patterned with relatively large heating units arranged in 2.5 mm-wide bands. After the substrate was tilted by $\sim 7^\circ$, the levitated IPA droplet ($\sim 40 \mu\text{L}$) was transported across a distance of 17.5 mm on the substrate in 0.27 s (i.e., $\sim 65 \text{ mm/s}$), indicating very low friction (Figure 1c). The Leidenfrost effect usually represents a metastable state of a droplet when it comes into contact with a surface that is significantly hotter than the liquid's boiling point. Typically, a vapor layer will be initialized for support and will thus yield a longer lifetime of the droplet and enable a virtually frictionless contact between the drop and substrate. The droplet transportation supported by an electrothermally actuated Leidenfrost effect is demonstrated for the first time in this report.

Actuation of the Leidenfrost effect was further investigated by designing and patterning micrometer-scaled heating arrays onto substrates. To quantitatively evaluate the electroheating actuation of the Leidenfrost effect, we designed the serpentine-shaped repeating unit cell (Figure 2a) to further reduce the surface coverage to 62.5% of the overall area of the heated region. A defined geometrical parameter, the heating ratio, is shown in the inset of Figure 2b, which is the 1-dimensional ratio $p:(p+d)$ between heated and unheated regions, where $p = 40 \mu\text{m}$ and represents the width of the heated region and d is the distance between consecutive unit cells. The total area heated for a given ratio can be calculated by multiplying the heated ratio by the serpentine unit cell coverage. For example, for a 0.2 heated ratio, the total heated percentage would be 20% multiplied by 62.5%, which is 12.5% of the area being heated. A typical plot of evaporation time versus input power on a heated two-dimensional array of unit cells (Figure 2b) is similar to previous results using more conventional methods (e.g., hot plate heated devices) (Figure S1). In Figure 2b, the Leidenfrost transition (dotted line) is monitored by recording the evaporation time of a droplet, t_{eva} , as a function of the power input for a 0.5 heated ratio array. The dotted line of 21.8 W is the typical power value needed to boil the IPA droplet (for

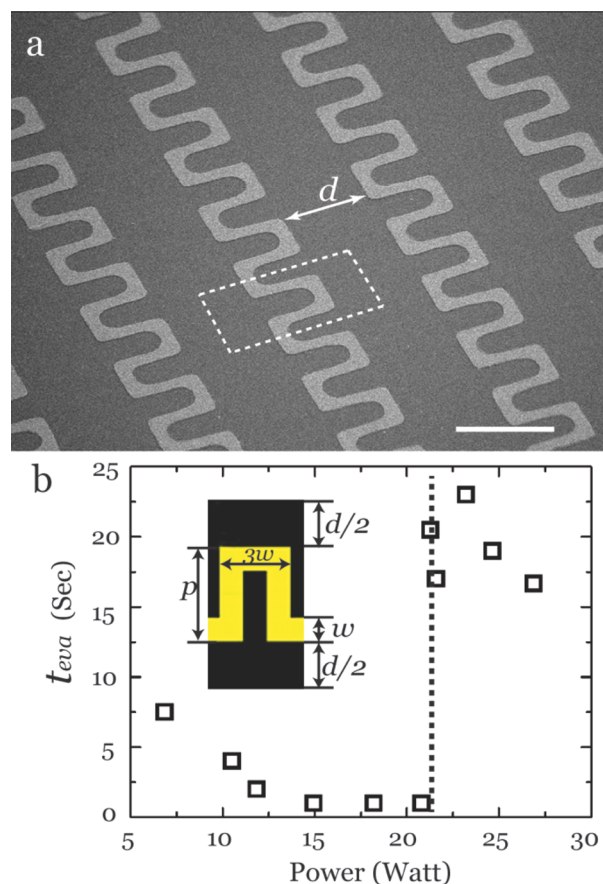


Figure 2. Micropattern of gold heating units and detection of the critical Leidenfrost transition. (a) SEM image of micropatterned chromium/gold heating array using serpentine patterns defined by an electrode width $w = 10 \mu\text{m}$, gap distance d , and electrode structure width $p = 40 \mu\text{m}$. (b) The Leidenfrost transition (dotted line) is monitored by recording the evaporation time of a droplet, t_{eva} , as a function of power input. The inset shows the unit cell design within a serpentine electrode for selective heating of the substrate (the heated area is the lighter area), where the overall unit area is shown by the dashed box in panel a.

these experiments, a $20 \mu\text{L}$ volume was used) for this heated ratio, whereby the IPA touches the hot surface and evaporates due to the high temperature of the surface below it. Above this power, the transition regime denotes a region where the substrate is hot enough to begin creating a localized vapor underneath the droplet, but the temperature is not yet high enough to do this in a stable way and the vapor layer is not thick enough to maintain a levitating droplet. In the stable Leidenfrost regime (right of the dotted line), the vapor can maintain a stable levitated state for the droplet. The determination of transition regime under selectively heated electrical actuation reveals a strong similarity to that from global heating of the substrate.

In contrast to heating a substrate globally, selective heating to create discontinuously heated fields across the in-plane area of the substrate should reduce the energy input. To understand how the thermal energy distributes across the substrate, we performed surface thermal analysis using COMSOL Multiphysics. The qualitative analysis (Figure 3a) first considers a serpentine unit cell resistor (0.2 heated ratio) on a borosilicate glass substrate with a voltage applied to show the temperature profile of the single unit cell above the Leidenfrost transition

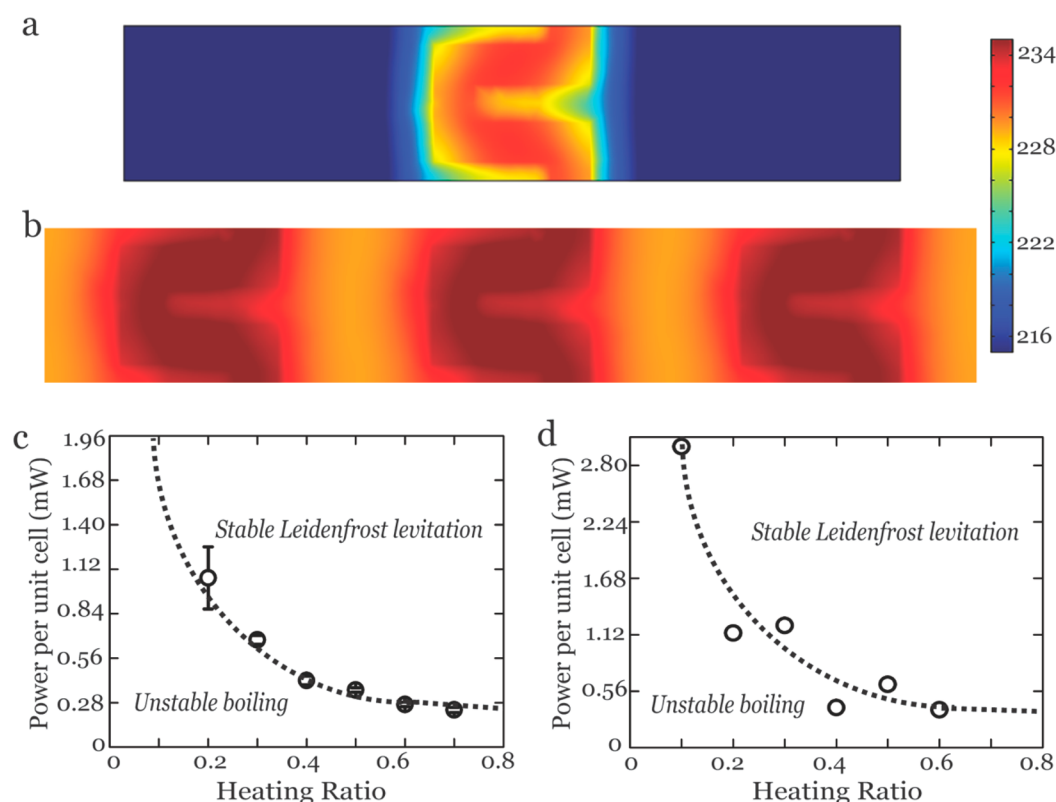


Figure 3. Selective Leidenfrost mechanism and phase diagrams. (a) Temperature profile of surface for the electroheating of single unit cell with a 0.2 heated ratio. The COMSOL simulation in panel b reveals a uniform distribution of the temperature ($^{\circ}\text{C}$) across the unit cells within three adjacent serpentine units (a heated ratio of 0.5). The simulation is based on 363 serpentine unit cells in a series, which is referred to as a line, and a number of these lines are connected in parallel to form a complete heating array. The applied voltage is then varied to provide an equivalent power per cell required for the Leidenfrost effect to occur. The selective Leidenfrost effect using this pattern is described by phase diagrams on (c) a glass substrate and (d) a silicon substrate. The dotted lines represent the simulation results and the symbols represent the experimental results, respectively.

temperature. The heat created as a result is then dissipated through the substrate, the stage underneath, and also through the air above the resistor. As can be seen in Figure 3a, the temperature difference across a distance of $100\ \mu\text{m}$, from the center of the heat to halfway between two unit cells (or a heated ratio of 0.2), is as high as $20\ ^{\circ}\text{C}$ for the borosilicate glass substrate.

As a result of this temperature difference, it would be expected that the resistors with a lower heated ratio (or a larger gap between them) would have to be heated to a higher temperature than required to get the coolest part of the array to still be hot enough for the Leidenfrost effect to occur. To prove this, we further simulated the unit cells with three adjacent serpentine units shown on the same substrate (Figure 3b) with a voltage applied on each unit cell (heated ratio = 0.5) and demonstrate a more uniform distribution of the temperature (the difference of temperature is less than $5\ ^{\circ}\text{C}$). In this case, the voltage required is lower than that for the unit cell shown in Figure 3a. We note that the current flow through the serpentine-shaped unit cell is nonuniform as a result of the structure's geometry, as can be seen in Figure S2, and the subsequent thermal stress localization could potentially lead to mechanical failure. However, no failures occurred in our experiment, and this may have been because the localized strain energy was likely absorbed by the in-plane structural expansion and the chromium adhesion layer.

Using the selectively heated substrate with repeated unit cells (heated ratio = 0.5), we next plotted the phase diagrams to describe the metastable state of the heated IPA droplet on a

glass substrate (Figure 3c) and a silicon substrate (Figure 3d). Experimental data are compared with the COMSOL simulation results. The Leidenfrost state is shown in the diagram, and the anticipated trend of reducing power required to initiate the Leidenfrost effect when increasing the heating ratio is observed. There is good agreement between the experimental and simulated results, where the model assumes a Leidenfrost temperature of $220\ ^{\circ}\text{C}$. This is a reasonable value for IPA, which has a boiling point of $82.4\ ^{\circ}\text{C}$.³⁴

As the selectivity of the Leidenfrost effect is via voltage actuated heating units on the substrate, the thermal conductivity of the latter has a direct influence on the results. Two substrate materials with a large difference on thermal conductivity were employed to verify this impact: borosilicate glass ($1.14\ \text{W/mK}$) and silicon ($1480\ \text{W/mK}$) at $300\ \text{K}$.³² As can be seen in Figure 3d, the results for a silicon substrate still follow the decreasing trend with an increasing heated ratio. However, a power per line greater than that for the borosilicate substrates is required to achieve the Leidenfrost effect because the heat is dissipated through the substrate more readily rather than remaining in the vicinity of the serpentine-shaped unit cells to form the uniform in-plane temperature profile. Therefore, borosilicate is a more preferable substrate material for this experiment as it could create a uniform temperature profile more effectively on the surface of the substrate owing to its low thermal conductivity.

Finally, we demonstrate the possibility of controlling droplet transportation by taking advantage of using a selectively heated substrate (Figure S3). A substrate with four separate blocks of

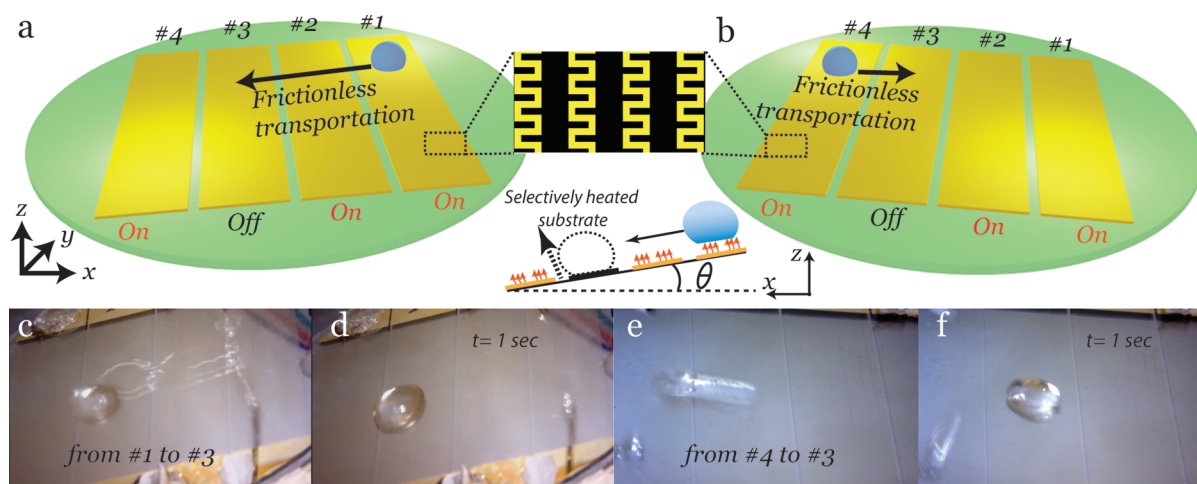


Figure 4. Demonstration of droplet transportation using programmable activation of localized heating units. (a and b) Schematic illustrations of experimental arrangements with example designs which selectively cover a substrate with four micropatterned heating arrays (numbered 1–4 from right to left); each complete unit consists of serpentine-patterned unit cells as illustrated by Figure 2a. The third unit is nonactivated to give an “off” state, while the others are activated into an “on” state. The whole wafer is tilted at a small angle of (a) 10° and (b) -10° , as shown in the inset side-view schematic. The droplet travels downslope across regions 1 and 2 with almost no friction due to the Leidenfrost effect but then stops when it reaches the nonactivated region 3; droplet transport is also stopped on the nonactivated region when the substrate tilt is reversed (b). (c) Momentary snapshot of the droplet transportation showing the droplet advancing from region 1 to region 3 with the setting in panel a and finally stopping at the nonactivated region 3 (d). (e and f) Experimental images for droplet transport records the rapid, virtually frictionless droplet transport from region 4 to 3 with the setting in panel b.

0.5 ratio heating arrays, each of which could be individually switched in sequence, was created, as seen in Figures 4a and b. The first, second, and fourth arrays were switched on for 0.1 s in turn with a 0.1 s time gap between each one being switched on. Therefore, the substrate was selectively heated in the microscale (due to the heated ratio), the macroscale (the four arrays being heated individually), and in time (the arrays being sequenced individually). Each array was activated for an eighth of a cycle. The third array was left disconnected. A schematic of the controlled droplet transportation shows the droplet to the target zone (unactivated region) possessing the disconnected heating array in a short time. Experimental images (Figures 4c and d) indicate rapid droplet movements from both directions to region 3 at a speed comparable to that witnessed in Figure 1c, thus implying rapid, virtually frictionless transport. This concept also enables a new strategy of targeted delivery of a droplet by configuring the substrate to form localized frictionless levitation layers on demand, which could be of considerable interest to scientists and researchers in microfluidic systems, chemical engineering, biological engineering, and other related areas.

CONCLUSION

In conclusion, we demonstrated the electroheating actuation of the Leidenfrost effect for three different liquids by applying voltages to heating units which selectively cover a substrate. This approach provides rapidly switchable and highly targeted transportation of a droplet according to the design of the geometry and layout of the heating array on the substrate. By the selective heating of a sample to produce the Leidenfrost effect in a small area where needed rather than using a hot plate to heat the entire surface, the same effect can be achieved but with a much lower energy requirement. It also provides the potential for easy integration to be part of an on-chip device with an electrical triggering mechanism. Moreover, further energy efficiency could be achieved by using a feedback control

system to drive and control the direction of motion of droplets with actuation of only those heating units in the immediate locality of the levitated droplet.

ASSOCIATED CONTENT

Supporting Information

The Supporting Information is available free of charge on the ACS Publications website at DOI: 10.1021/acsami.6b06738.

Leidenfrost transition graph for a sample on a hot plate (Figure S1) and COMSOL image of current flow through a serpentine resistor on a borosilicate substrate (Figure S2) (PDF)

Video of targeted transportation of a droplet on a selectively heated substrate (AVI)

AUTHOR INFORMATION

Corresponding Author

*E-mail: l.e.dodd@durham.ac.uk.

Notes

The authors declare no competing financial interest.

ACKNOWLEDGMENTS

The work was supported by the Engineering and Physical Sciences Research Council (EPSRC) through grants EP/L026899/1, EP/L026619/1, and EP/L026341/1. The authors also acknowledge funding from the EU-COST MP1106 network.

REFERENCES

- (1) Bhushan, B.; Jung, Y. C. Natural and Biomimetic Artificial Surfaces for Superhydrophobicity, Self-Cleaning, Low Adhesion, and Drag Reduction. *Prog. Mater. Sci.* **2011**, *56*, 1–108.
- (2) Liu, K.; Jiang, L. Bio-Inspired Self-Cleaning Surfaces. *Annu. Rev. Mater. Res.* **2012**, *42*, 231–263.
- (3) Zhao, B.; Moore, J. S.; Beebe, D. J. Surface-Directed Liquid Flow Inside Microchannels. *Science* **2001**, *291*, 1023–1026.

- (4) Yao, X.; Song, Y.; Jiang, L. Applications of Bio-Inspired Special Wettable Surfaces. *Adv. Mater.* **2011**, *23*, 719–734.
- (5) Ionov, L.; Houbenov, N.; Sidorenko, A.; Stamm, M.; Minko, S. Smart Microfluidic Channels. *Adv. Funct. Mater.* **2006**, *16*, 1153–1160.
- (6) Feng, L.; Li, S.; Li, Y.; Li, H.; Zhang, L.; Zhai, J.; Song, Y.; Liu, B.; Jiang, L.; Zhu, D. Super-Hydrophobic Surfaces: From Natural to Artificial. *Adv. Mater.* **2002**, *14*, 1857–1860.
- (7) Zheng, Y.; Gao, X.; Jiang, L. Directional Adhesion of Superhydrophobic Butterfly Wings. *Soft Matter* **2007**, *3*, 178–182.
- (8) Zhang, J.; Han, Y. Shape-Gradient Composite Surfaces: Water Droplets Move Uphill. *Langmuir* **2007**, *23*, 6136–6141.
- (9) Bliznyuk, O.; Seddon, J. R. T.; Veligura, V.; Kooij, E. S.; Zandvliet, H. J. W.; Poelsema, B. Directional Liquid Spreading over Chemically Defined Radial Wettability Gradients. *ACS Appl. Mater. Interfaces* **2012**, *4*, 4141–4148.
- (10) Kim, P.; Kreder, M. J.; Alvarenga, J.; Aizenberg, J. Hierarchical or Not? Effect of the Length Scale and Hierarchy of the Surface Roughness on Omniphobicity of Lubricant-Infused Substrates. *Nano Lett.* **2013**, *13*, 1793–1799.
- (11) Smith, J. D.; Dhiman, R.; Anand, S.; Reza-Garduno, E.; Cohen, R. E.; McKinley, R. H.; Varanasi, K. K. Droplet Mobility on Lubricant-Impregnated Surfaces. *Soft Matter* **2013**, *9*, 1772–1780.
- (12) Yao, X.; Hu, Y.; Grinthal, A.; Wong, T. S.; Mahadevan, L.; Aizenberg, J. Adaptive Fluid-Infused Porous Films with Tunable Transparency and Wettability. *Nat. Mater.* **2013**, *12*, 529–534.
- (13) Chaudhury, M. K.; Whitesides, G. M. How To Make Water Run Uphill. *Science* **1992**, *256*, 1539–1541.
- (14) Ghosh, A.; Ganguly, R.; Schutzius, T. M.; Megaridis, C. M. Wettability Patterning for High-Rate, Pumpless Fluid Transport on Open, Non-Planar Microfluidic Platforms. *Lab Chip* **2014**, *14*, 1538–1550.
- (15) Lv, C.; Chen, C.; Chuang, Y. C.; Tseng, F. G.; Yin, Y.; Grey, F.; Zheng, Q. Substrate Curvature Gradient Drives Rapid Droplet Motion. *Phys. Rev. Lett.* **2014**, *113*, 026101.
- (16) Leidenfrost, J. G. On Fixation of Water in Diverse Fire. *Int. J. Heat Mass Transfer* **1966**, *9*, 1153 (translated by C. Wares).
- (17) Biance, A. L.; Clanet, C.; Quéré, D. Leidenfrost Drops. *Phys. Fluids* **2003**, *15*, 1632.
- (18) Dupeux, G.; Le Merrer, M.; Clanet, C.; Quéré, D. Trapping Leidenfrost Drops with Crenulations. *Phys. Rev. Lett.* **2011**, *107*, 114503.
- (19) Dupeux, G.; Le Merrer, M.; Lagubeau, G.; Clanet, C.; Hardt, S.; Quéré, D. Viscous Mechanism for Leidenfrost Propulsion on a Ratchet. *EPL* **2011**, *96*, 58001.
- (20) Celestini, F.; Frisch, T.; Pomeau, Y. Take Off of Small Leidenfrost Droplets. *Phys. Rev. Lett.* **2012**, *109*, 034501.
- (21) Dupeux, G.; Bourriane, P.; Magdelaine, Q.; Clanet, C.; Quéré, D. Propulsion on a Superhydrophobic Ratchet. *Sci. Rep.* **2014**, *4*, 5280.
- (22) Quéré, D. Leidenfrost Dynamics. *Annu. Rev. Fluid Mech.* **2013**, *45*, 197–215.
- (23) Wells, G. G.; Ledesma-Aguilar, R.; McHale, G.; Sefiane, K. A Sublimation Heat Engine. *Nat. Commun.* **2015**, *6*, 6390.
- (24) Vakarelski, I. U.; Patankar, N. A.; Marston, J. O.; Chan, D. Y. C.; Thoroddsen, S. T. Stabilization of Leidenfrost Vapour Layer by Textured Superhydrophobic Surfaces. *Nature* **2012**, *489*, 274–277.
- (25) Vakarelski, I. U.; Marston, J. O.; Chan, D. Y. C.; Thoroddsen, S. T. Drag Reduction by Leidenfrost Vapor Layers. *Phys. Rev. Lett.* **2011**, *106*, 214501.
- (26) Lagubeau, G.; Le Merrer, M.; Clanet, C.; Quéré, D. Leidenfrost on a Ratchet. *Nat. Phys.* **2011**, *7*, 395–398.
- (27) Ok, J. T.; Lopezona, E.; Nikitopoulos, D. E.; Wong, H.; Park, S. Propulsion of Droplets on Micro- and Sub-Micron Ratchet Surfaces in the Leidenfrost Temperature Regime. *Microfluid. Nanofluid.* **2011**, *10*, 1045–1054.
- (28) Feng, R.; Zhao, W.; Wu, X.; Xue, Q. Ratchet Composite Thin Film for Low-Temperature Self-Propelled Leidenfrost Droplet. *J. Colloid Interface Sci.* **2012**, *367*, 450–454.
- (29) Galdi, N. R.; McHale, G.; Xu, B. B.; Wells, G. G.; Dodd, L. E.; Wood, D.; Newton, M. I. Leidenfrost Transition Temperature for Stainless Steel Meshes. *Mater. Lett.* **2016**, *176*, 205–208.
- (30) Piroird, K.; Clanet, C.; Quéré, D. Magnetic Control of Leidenfrost Drops. *Phys. Rev. E: Stat., Nonlinear, and Soft Matter Phys.* **2012**, *85*, 056311.
- (31) Wang, Y.; Bhushan, B. Liquid Microdroplet Sliding on Hydrophobic Surfaces in the Presence of an Electric Field. *Langmuir* **2010**, *26*, 4013–4017.
- (32) Ng, B. T.; Hung, Y. M.; Tan, M. K. Acoustically-Controlled Leidenfrost Droplets. *J. Colloid Interface Sci.* **2016**, *465*, 26–32.
- (33) Linke, H.; Alemán, B. J.; Melling, L. D.; Taormina, M. J.; Francis, M. J.; Dow-Hygelund, C. C.; Narayanan, V.; Taylor, R. P.; Stout, A. Self-Propelled Leidenfrost Droplets. *Phys. Rev. Lett.* **2006**, *96*, 154502.
- (34) Lide, D. R. *CRC Handbook of Chemistry and Physics*, 74th ed.; CRC Press, 1993.